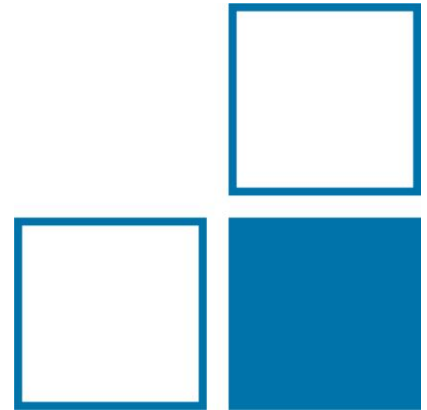

Instruments for High-Energy Neutron Metrology

R. Nolte



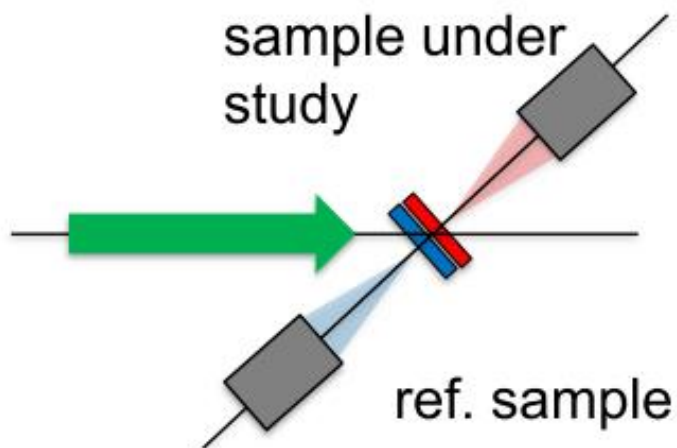
Overview

- Introduction: Properties of high-energy reference neutron beams
- Primary and secondary standard instruments
 - Reference cross sections
 - Recoil proton detectors
 - Fission detectors
- Alternative: Foil activation
- Ancillary equipment
 - Intensity monitors
 - Collimator design
 - Beam profile monitors
 - Scanning devices
- Summary

NB: Most of the examples are from work with PTB participation, simply because this is what I know best.

There is plenty of other excellent work outside!

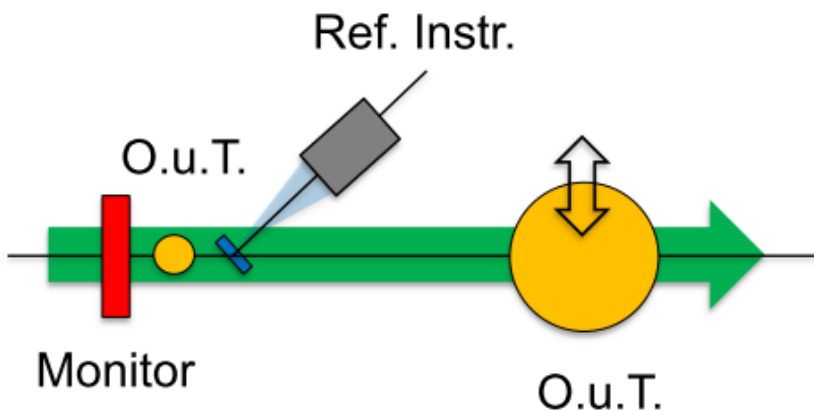
Specific Challenges for Reference Beams



Cross section measurement

- matched samples ('back-to-back')
- identical geometries and detectors for both samples
- constant beam intensities
- many effects cancel out

⇒ 'as relative as possible!'

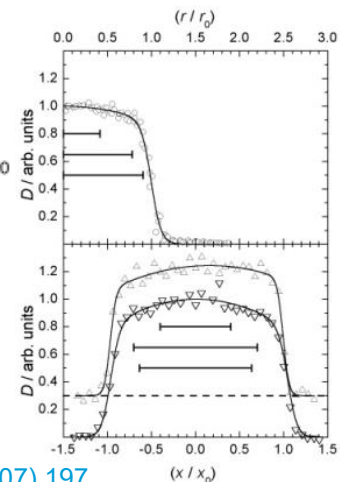
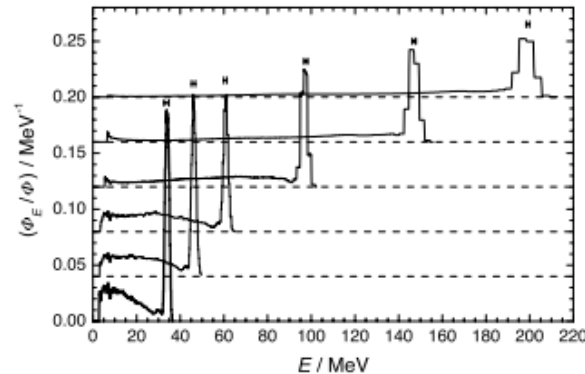
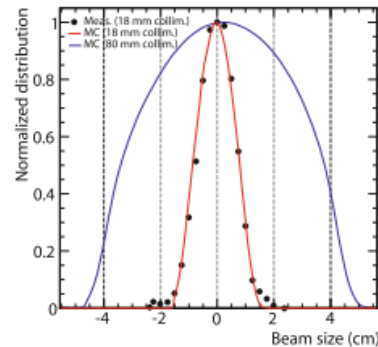
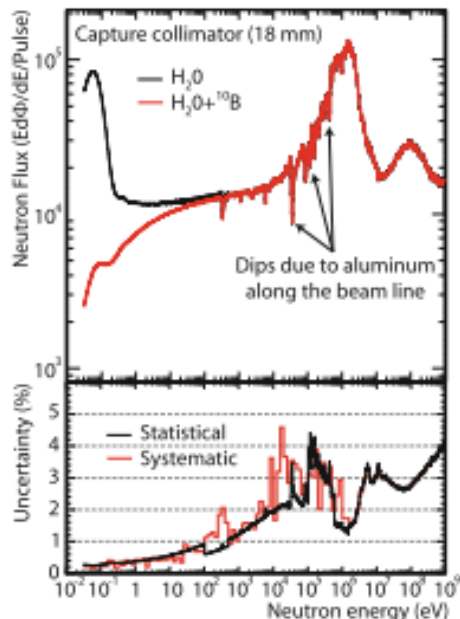


Reference Beam

- reference instrument and objects under test (O.u.T.) are different: **nucl. physics detector vs. dosimeter**
- beam intensity must be varied
- several 'good' monitors required
- scanning procedure may be needed

Properties of High-Energy Neutron Sources

Energy distribution:	quasi-monoenergetic: 'white':	Li+p, Be+p, Be+d, ... W+p, Pb+p, ...
Time distribution:	continuous: rep. rate:	DC - ns-pulsed 1 Hz - 10 MHz
Spatial distribution:	collimated beam: (divergent fields:	1 cm - 10 cm 4π)



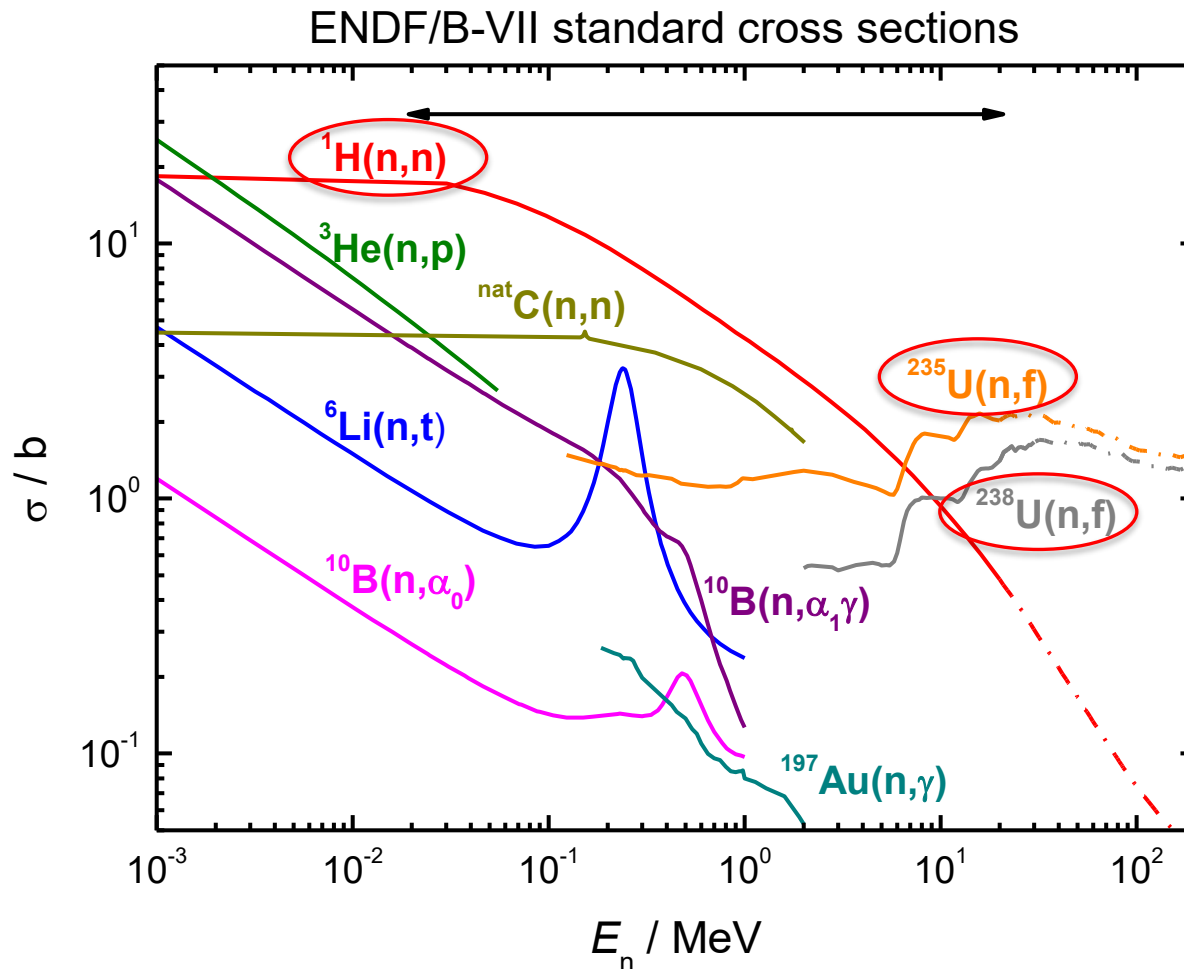
Ref.: C. Guerrero *et al.*, EPJA **49** (2013) 27

Ref.: R. Nolte *et al.*, NSE **156** (2007) 197

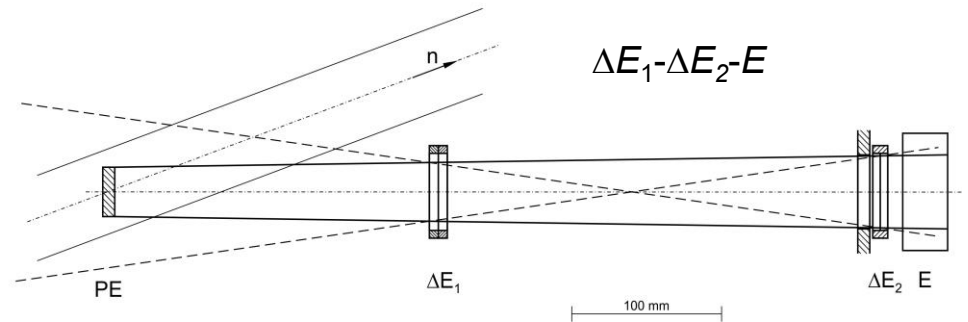
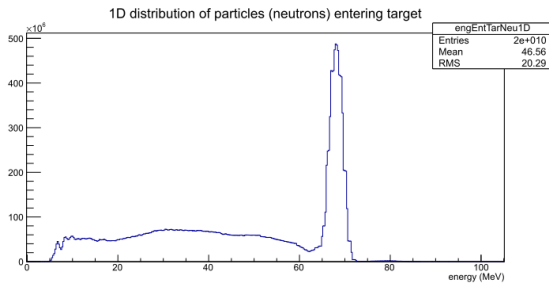
Cross Section Standards

Characterization rel. to primary or secondary standard cross sections:

$^1\text{H}(n,n)p$, $^{235,238}\text{U}(n,f)$



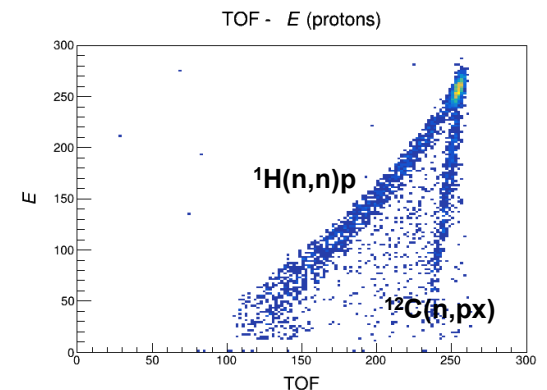
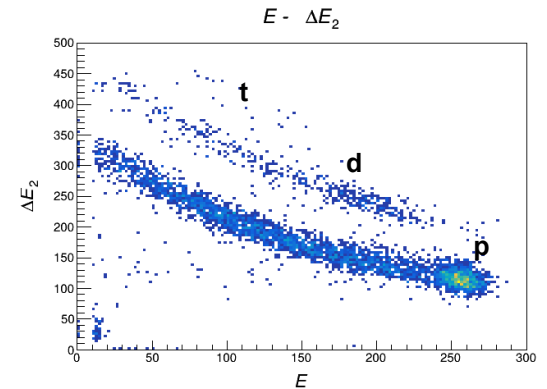
Recoil Proton Detectors: Telescopes



$$E_p \approx E_n \cos^2(\Theta_p), \quad d\sigma_{np}/d\Omega_p \approx \sigma_{np}/4\pi \cos(\Theta_p)$$

\Rightarrow Choose angle Θ_p close to 0° !

0.5 mm Si – 0.5 mm Si – 3" NaI



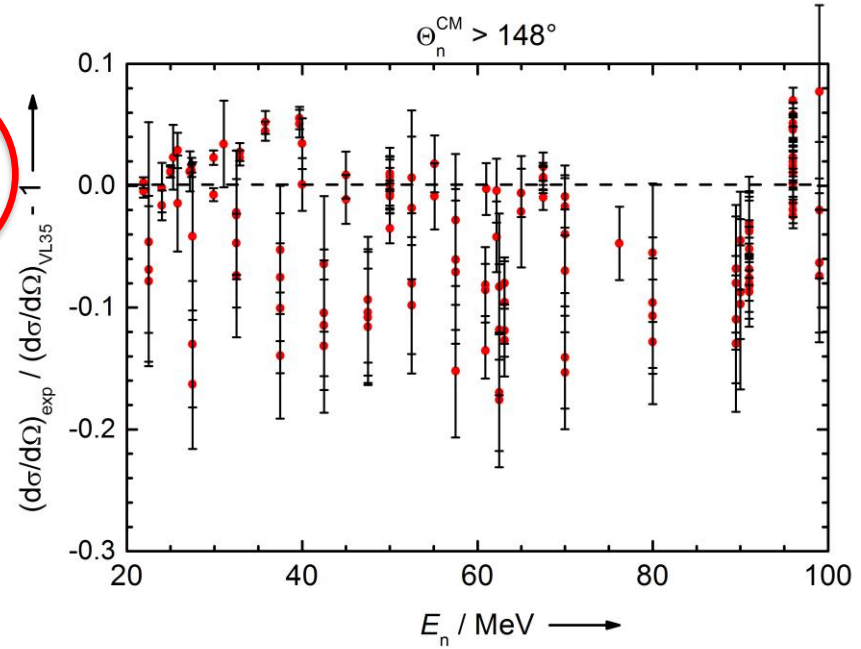
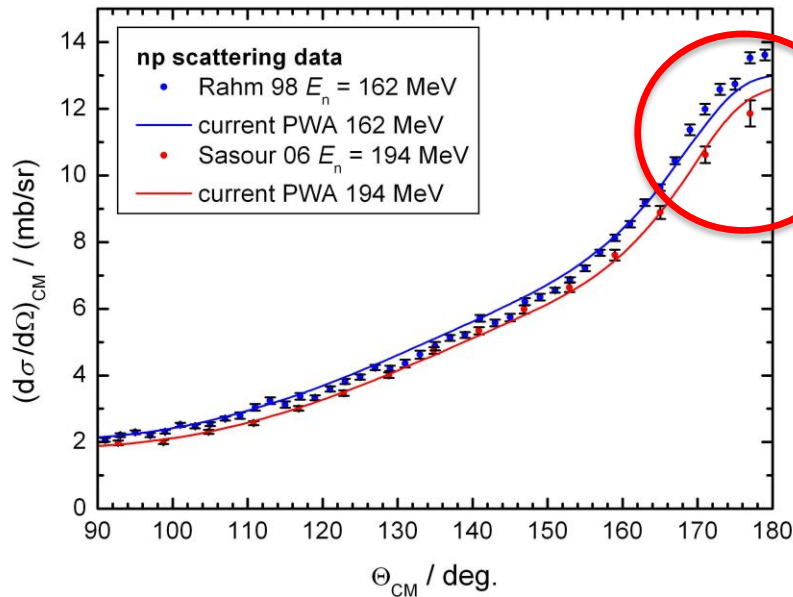
- Triple coincidence reduces background
- Particle identification: ΔE -E technique
- $^{12}\text{C}(n,px)$: matched graphite sample
- Energy distribution: Time-of-Flight (TOF) method

Dominant uncertainty contributions:

- Statistics: $\varepsilon_n \approx 10^{-3} - 10^{-4}$!
- Hydrogen content of PE samples: CH_x
- Diff. np scattering cross section: $(d\sigma_{np}/\Omega_p)$

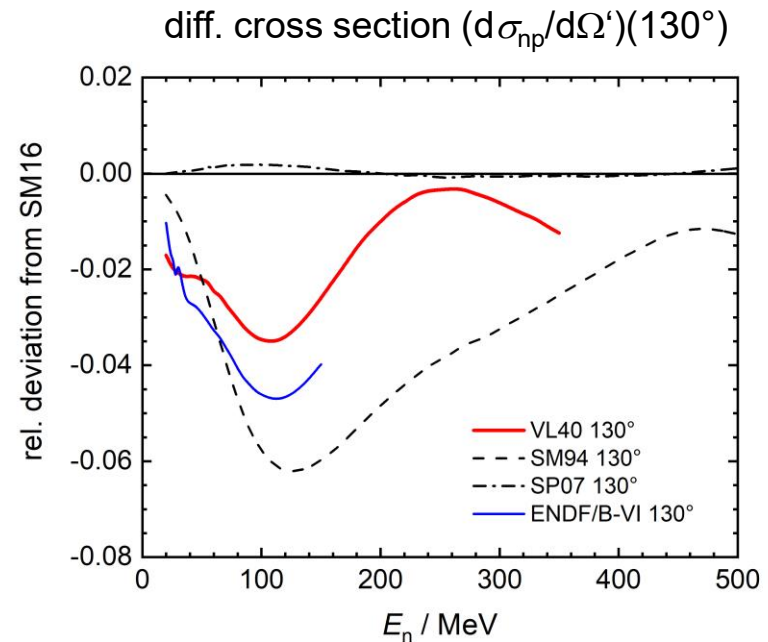
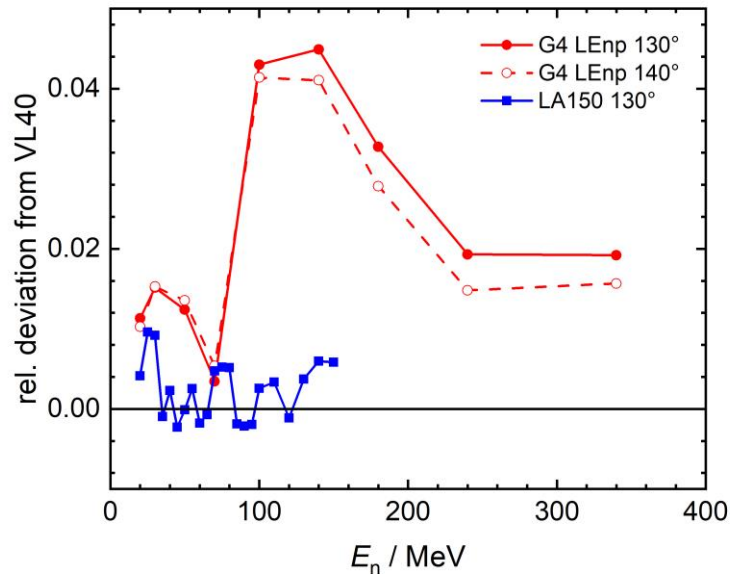
Reference Cross Section: $^1\text{H}(n,n)p$

n-p backward scattering



- Partial wave analysis (SAID code): <https://gwdac.phys.gwu.edu/>
- Recommended partial wave analysis: **VL40** (1996, $E_n < 400$ MeV)
- Data base contains many POL data from the 1980s -1990s, but only few new DX data above 30 MeV: FZK (90), UCL(97), TSL(91-05), IUCF (04-05)
- No uncertainties for DX from PWA: **'about 2%' - 'about 5%'**

Cross Sections for Monte Carlo Simulation of RPTs



Standard simulation tools: **MCNPX** (PTRAC) and **Geant4**

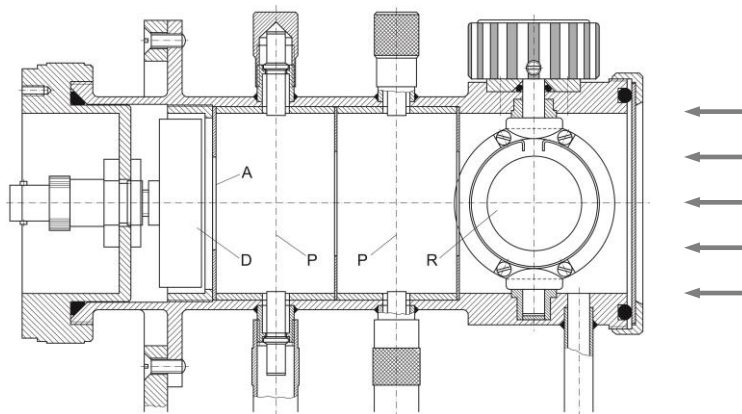
n-p cross section data bases:

- IAEA recommendation: still **PWA VL40** (1996)
- MCNPX: LA150 (almost VL40) and ENDF/B-VI (1997)
- Geant4: 'Results are extracted from R. Arndt's PSA of 1998'

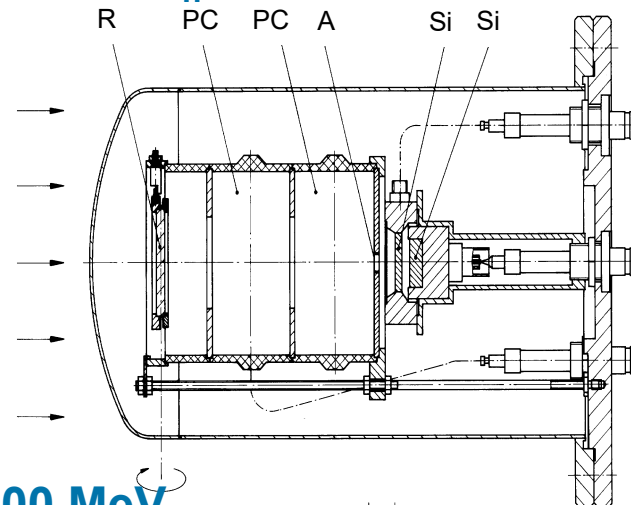
NB: π_0 production threshold at $E_n = 280$ MeV $\Rightarrow \sigma_{np} < \sigma_{tot}$

RPTs used at PTB over 40 Years

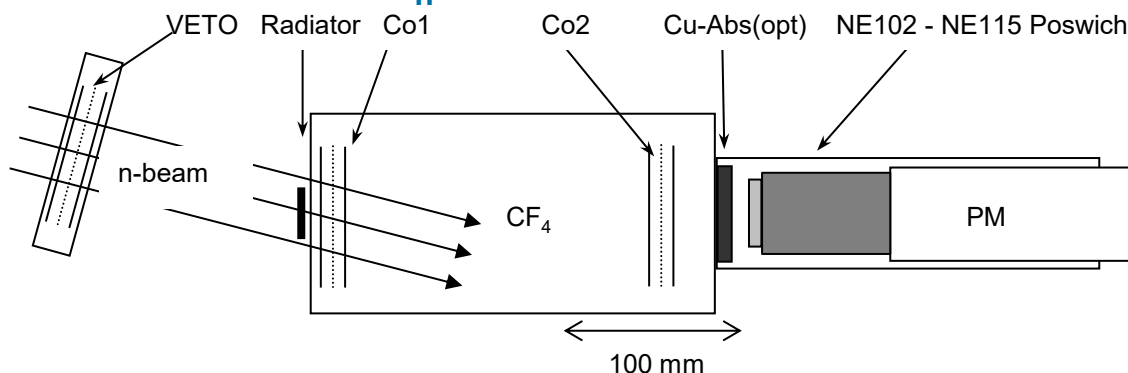
RPT1 $E_n = 1.5 \text{ MeV} - 20 \text{ MeV}$



RPT2 $E_n = 20 \text{ MeV} - 70 \text{ MeV}$



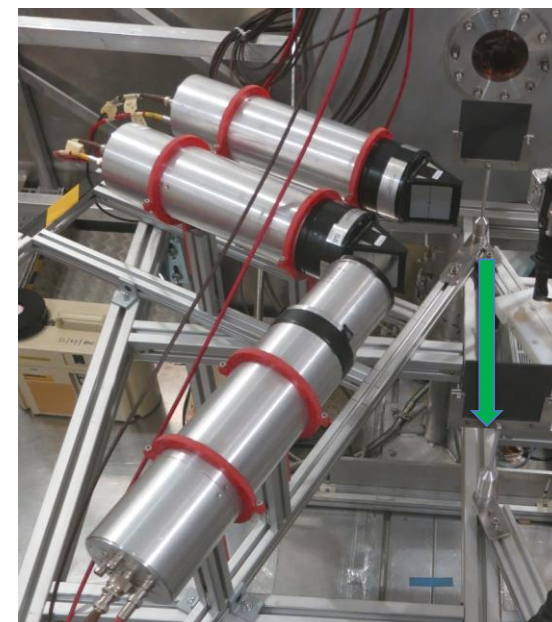
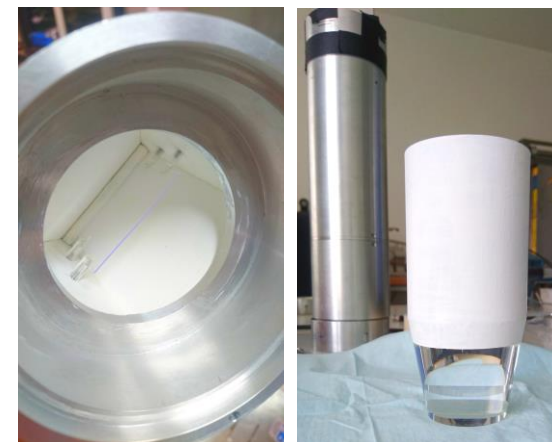
RPT3 $E_n = 40 \text{ MeV} - 200 \text{ MeV}$



- RPT1-2: $\Theta'_n = 180^\circ$, RPT3: $\Theta'_n = 150^\circ$
- Tristearine (RPT1) and PE (RPT2-3) radiators
- Particle identification: ΔE - E technique
- Coincidence requirement: 3-fold – 4-fold

The PTB RPT for n_TOF EAR1

- designed for 'white' beams: **TOF**
- plastic scintillators (EJ-204) + XP2020Q PMTs: **fast signals**
- triple stage: $\Delta E_1 - \Delta E_2 - E$: **low background**
- solid angle defined by size of ΔE_2
- particle identification via $\Delta E_2 - E$
- for fully-stopped particles: **clear sign. for n-p evt.s**
- polyethylene samples + matched graphite samples: **subtract. $^{12}\text{C}(\text{n,p})$ evt.s**
- Simulation with MCNPX: **n-p DX from VL40 PWA**



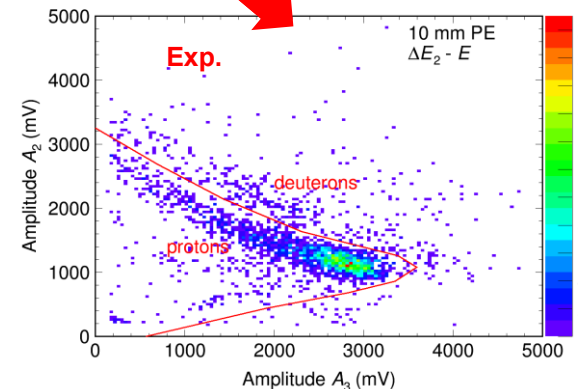
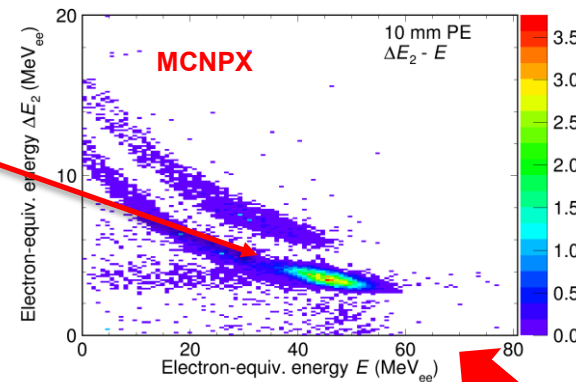
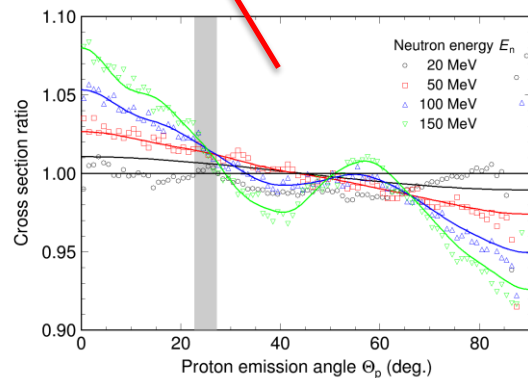
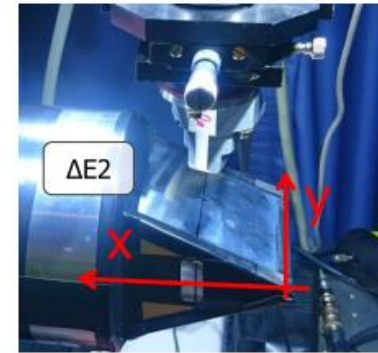
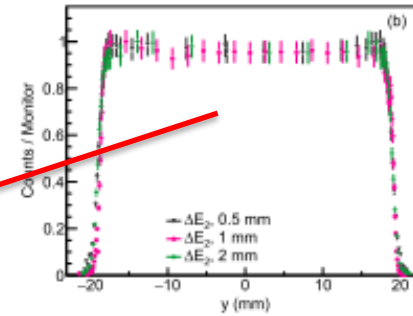
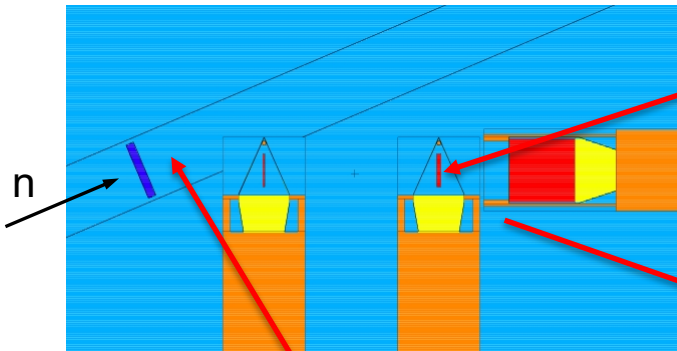
E_n / MeV	thickness / mm				
	ΔE_1	ΔE_2	E	CH_2	C
30 - 80	0.5	0.5	50	1	0.5
35 - 100	1	1	50	2	1
50 - 150	2	2	100	5	2.5

Ref.: E. Pirovano *et al.* JINST **18** (2023) P11011

n_TOF RPT: Simulation with MCNPX

Effective area of the ΔE_2 detector:

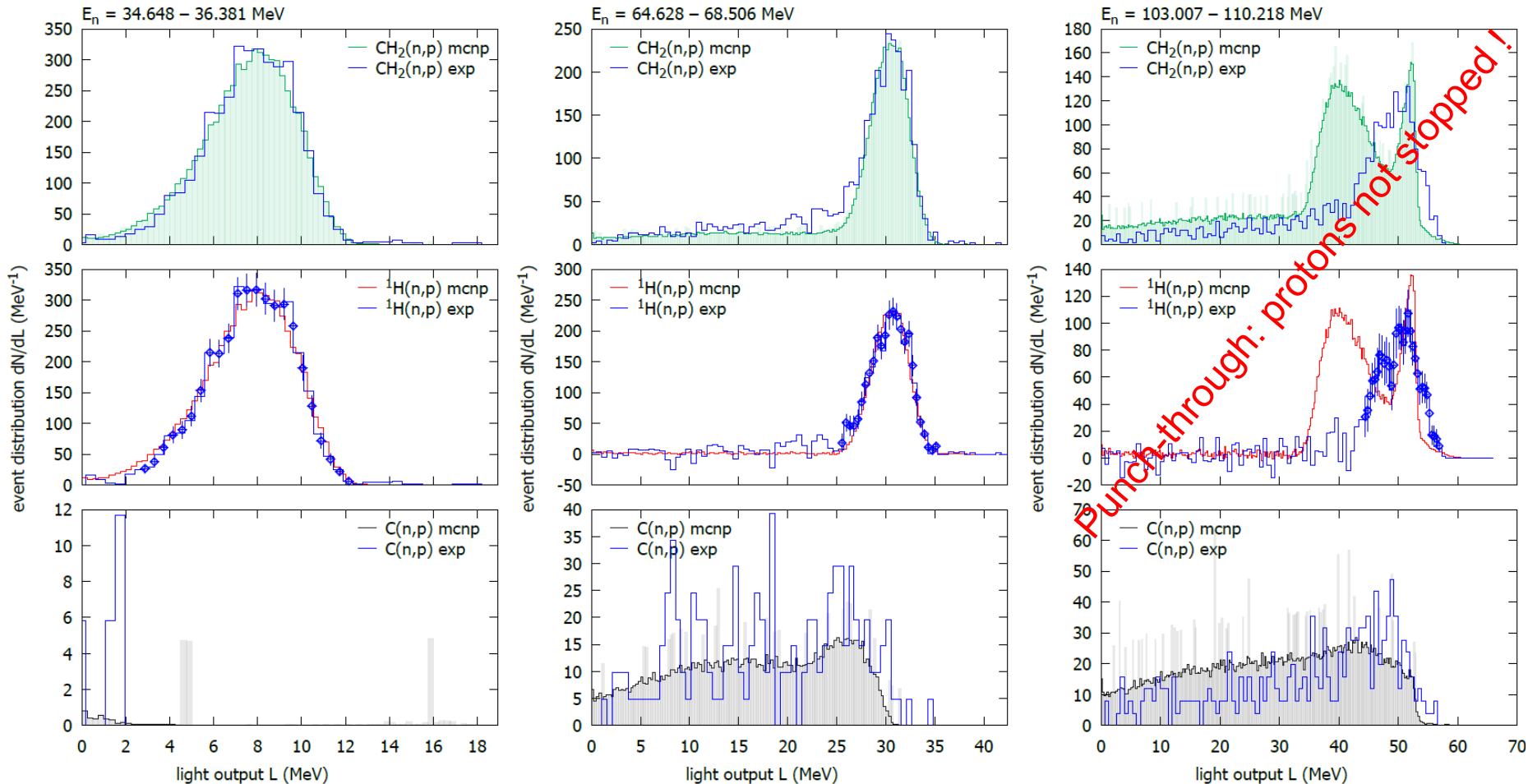
- Scan at the PTB micro ion beam
- Input for MCNPX simulation



NB: MCNPX uses non-relativistic kinematics:

⇒ Correction $k_{rel} = (d\Omega_p^{n.rel}/d\Omega_p^{rel})(E_n, \Theta_p)$ required

n_TOF RPT: Simulation vs. Experiment



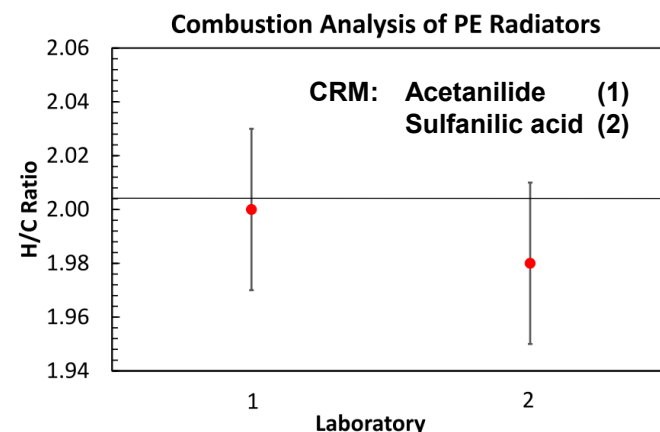
Net PH distributions after subtraction of the data from the graphite sample

The n_TOF RPT: Uncertainty Budget

Table 5. Systematic uncertainties affecting the neutron fluence measurement with the RPT. The values correspond to the uncertainty on the detection efficiency.

Contribution	Uncertainty
Beam transmission through PPFC, PPAC	0.5 %
Isotopic composition of PE	1.5 %
Areal density of PE sample	0.2-0.6 %
Areal density of C sample	0.2-0.9 %
Cuts the ΔE - E matrix for selecting proton events	0.5 %
Fit of MCNPX simulations to the experimental light-output distributions	≤ 2.5 %
Effective area of the ΔE_2 detector	0.5 %
Distance of the detectors from the PE or C sample	0.8 %
Angle relative to the neutron beam	0.1-0.6 %
Dead-time correction	0.5-1.0 %

Ref.: E. Pirovano *et al.* JINST **18** (2023) P11011



Present technical limit:

$$u_{H/C} \approx 0.8\%$$

Ref.: D. VanLeeuw, JRNC **305** (2015) 967

Dominating uncertainty contributions:

- Fit of the MCNPX sim.: fit region etc.
- PE Stoichiometry: CH_x
- np DX: $\approx 2\%$



excluded from uncertainty budget!

Recoil Proton Detectors: The TIARA RPT

Minimum uncertainty of the n-p DX expected at backward angles:

⇒ RPT with shadow bar and annular radiator: $\overline{\theta}'_n \approx 180^\circ$

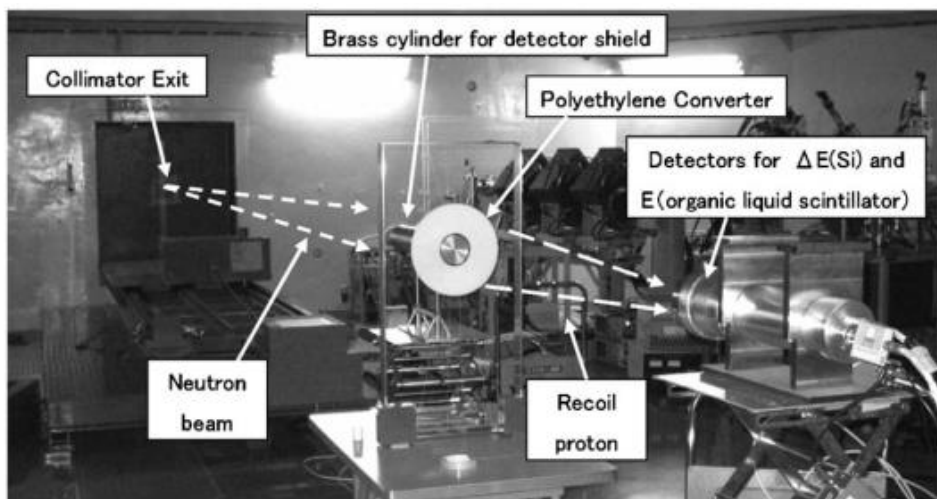


Fig. 2. Layout of the PRT componentry used to make absolute measurements in the neutron irradiation room at TIARA.

Table 2

Error sources and percentages used in the evaluation of the neutron fluence through absolute measurements made with the PRT at TIARA.

Error source	Relative error (%)
Count statistics	1.0–1.5
n-p scattering cross-section	5.0
Detection efficiency calculation statistics	1.4–2.0
Geometry	1.1–1.2
Beam monitor statistics	1.4–1.8
Normalization of beam current	2.6
Total	6.2–6.5

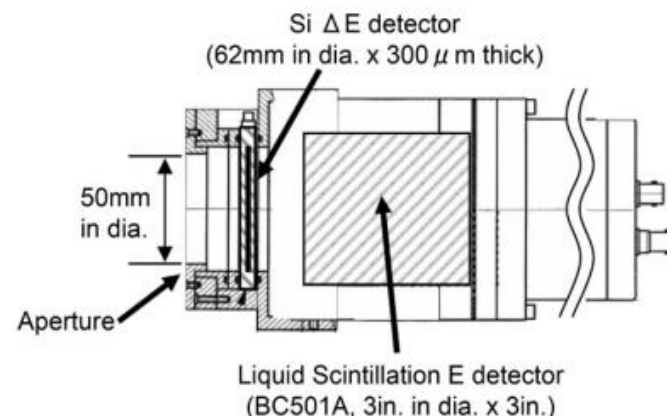


Fig. 3. Schematic view of the PRT detectors.

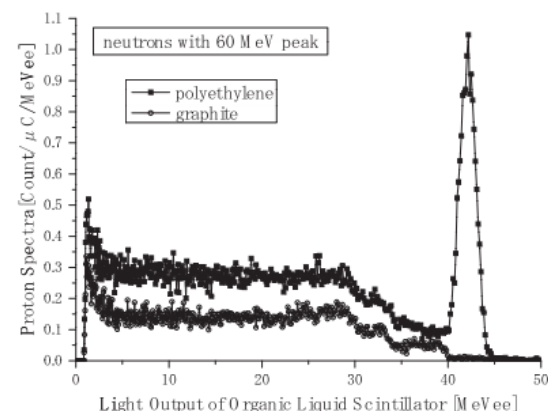
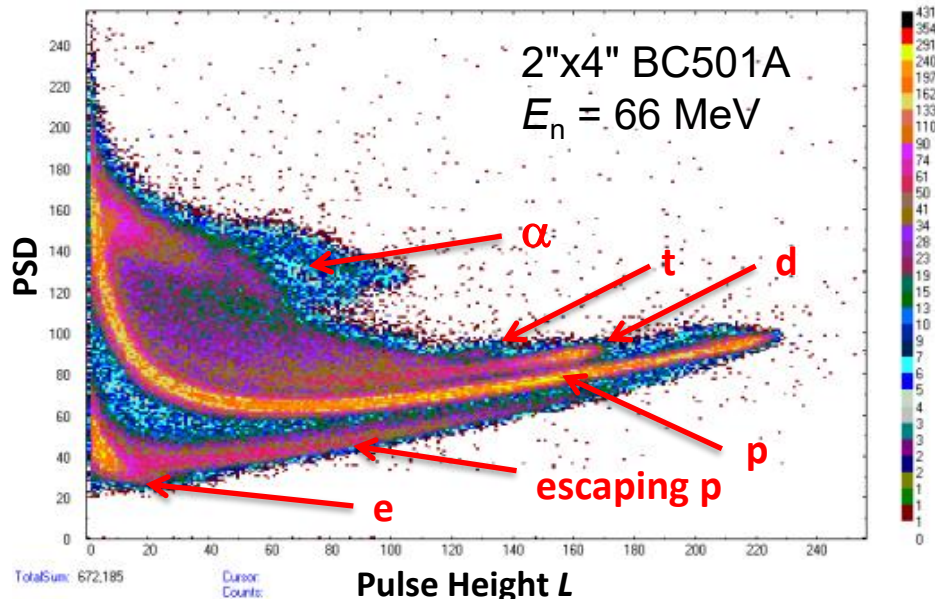
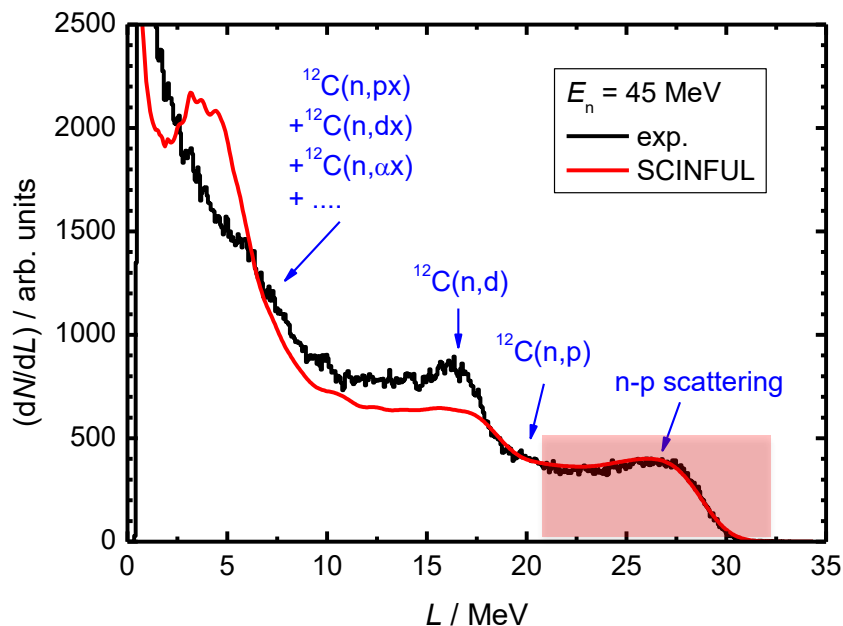


Fig. 6. Proton spectra for polyethylene and graphite converters for neutrons with 60 MeV peak.

Ref.: Y. Shikaze *et al.*, NIMA **615** (2010) 211-219

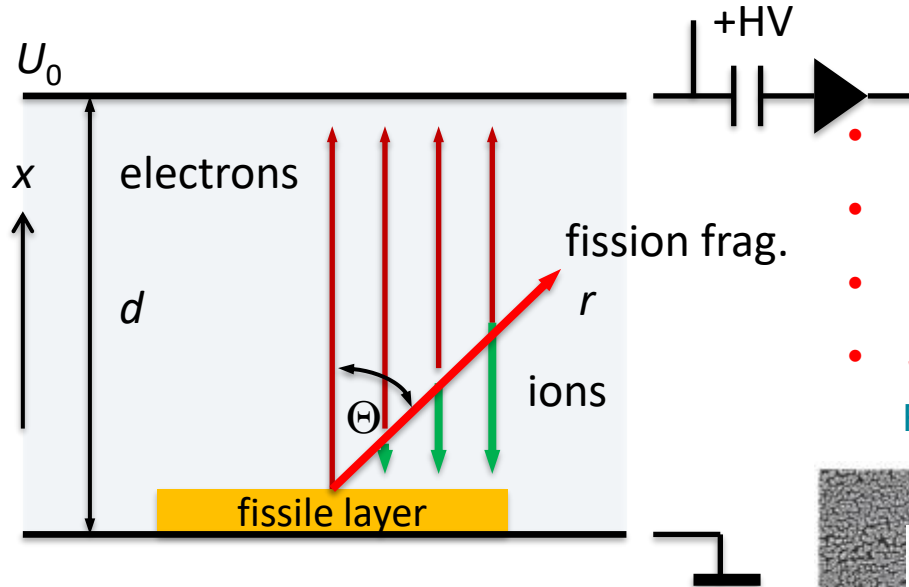
Recoil Proton Detectors: Scintillators



- Response dominated by n- ^{12}C interaction,
Data libraries (ENDF, JEFF) have only emission tables:
⇒ general-purpose MC codes are not sufficient: MCNPX, Geant4
- Workarounds:
 - variable PH threshold $L_0(E_n)$, **only $^1\text{H}(n,n)p$ events** (works for $E_n < 100$ MeV)
 - normalize efficiency for a fixed threshold L_0 : **work at RIKEN facility**

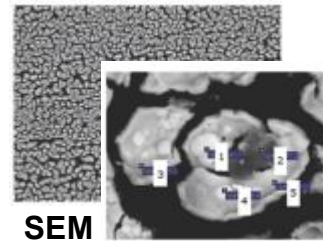
Ref.: N. Nakao *et al.*, NIMA **420** (1999) 218-231

Fission Detectors: Parallel-Plate Ionization Chambers



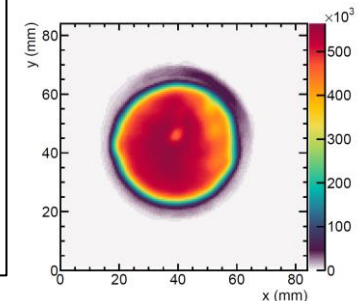
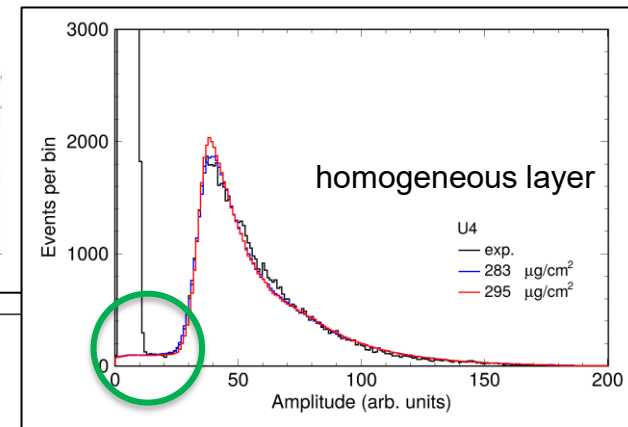
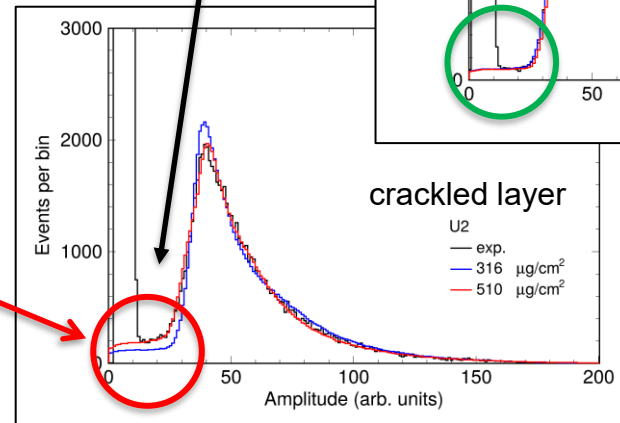
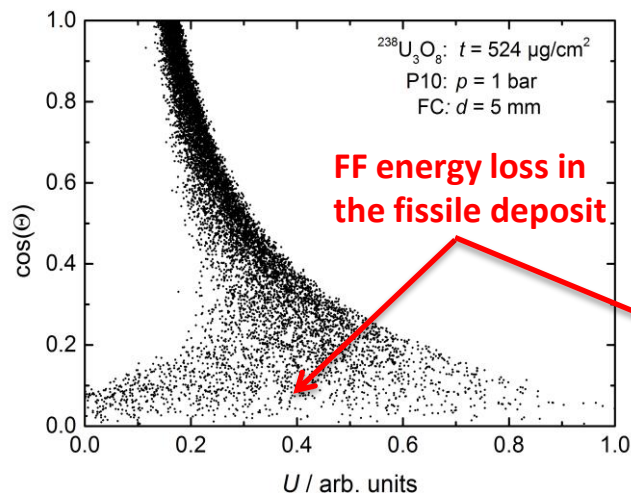
- Fragment detection eff.: $\varepsilon_f \approx 90\% - 95\%$
- Neutron detection eff.: $\varepsilon_n \approx 10^{-4}$
- Number of fiss. target nuclei: α -counting
- **Sample quality is crucial!**

Ref.: A. Vascon *et al.* NIMA **714** (2013) 163

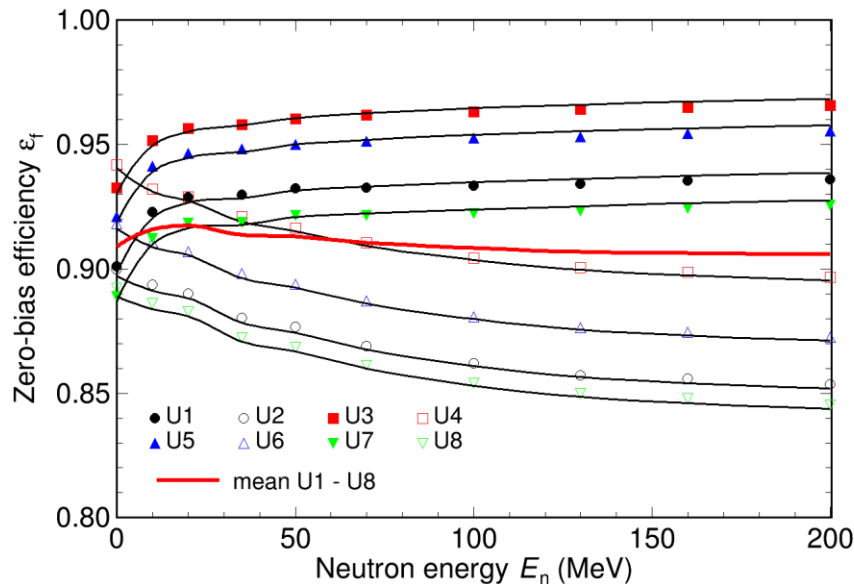


SEM

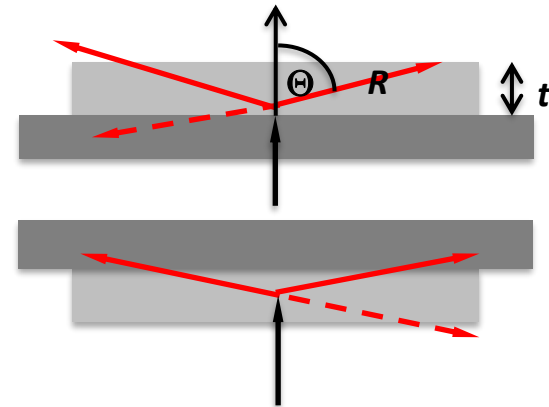
Monte Carlo Simulation



Fission Fragment Detection Efficiency



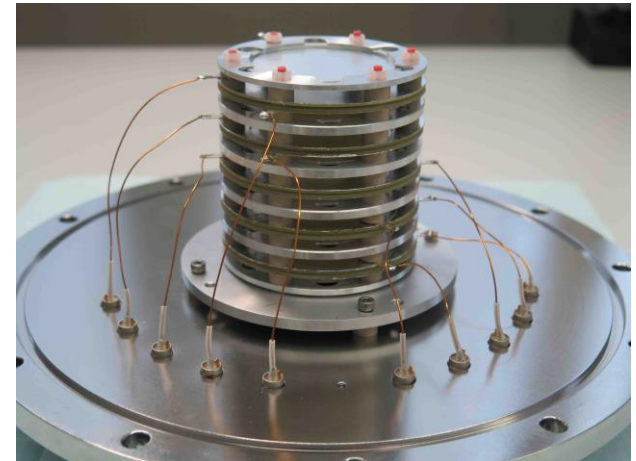
Effect of sample orientation



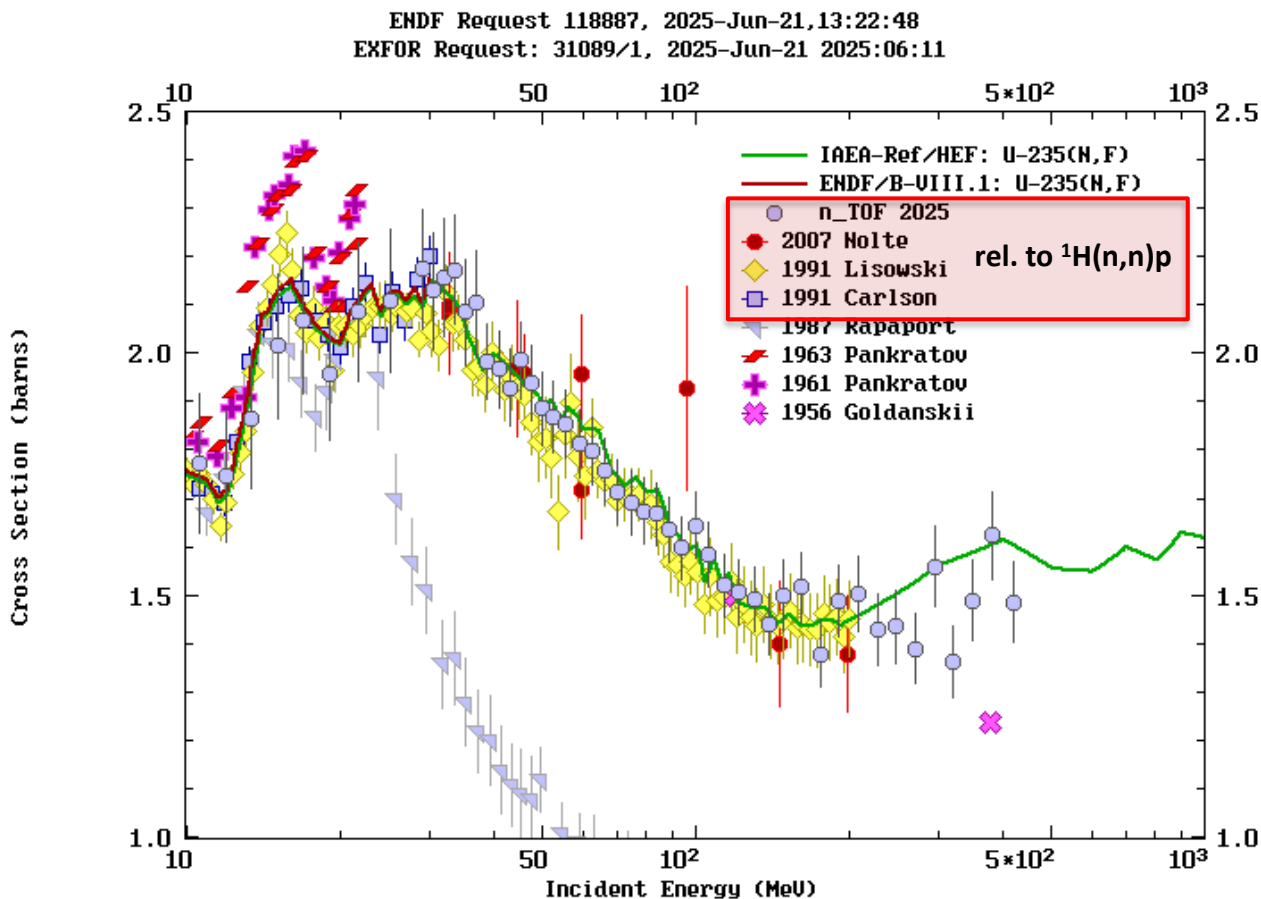
^{235}U PPFC used at n_TOF

Efficiency determined by:

- thickness and homogeneity of the deposit
 - partial transfer of linear momentum
 - angular distribution of fission fragments
- ⇒ Energy independence by combining forward- and backward-oriented samples



Reference Cross Section: $^{235}\text{U}(n,f)$



- Experimental data above 20 MeV available in EXFOR
- New n_TOF measurement confirms LANL+NIST data (1991 Lisowski, 1991 Carlson)
- Data base extended to 450 MeV

The Harwell FCs and n_TOF PPFC: Uncertainty Budget

Contributions to the Standard Measurement Uncertainty of the Fission Cross Sections*

Source of Uncertainty	Typical Relative Uncertainty	Type
Number of fissionable nuclei, N_n	0.002 to 0.005	A
Chamber efficiency, ε	0.016	B
Number of fission events, N_f	0.01 to 0.05	A
Peak fluence, Φ_0	0.025 to 0.035	B
Monitor reading, M	0.02	B
Correction factor, k_1	0.007	B
Correction factor, k_2	0.009	B
Correction factor, k_3	0.004	B
Correction factor, k_4	0.002	B
Correction factor, k_5	0.003	B
Correction factor, k_6	0.013	B
Correction factor, k_7	0.01 to 0.07	B

Ref.: R. Nolte *et al.* NSE **156** (2007) 197

Table 4. Systematic uncertainties affecting the fission-rate measurements with the PPFC. They were calculated both for each uranium target separately ('single deposit') and for the average.

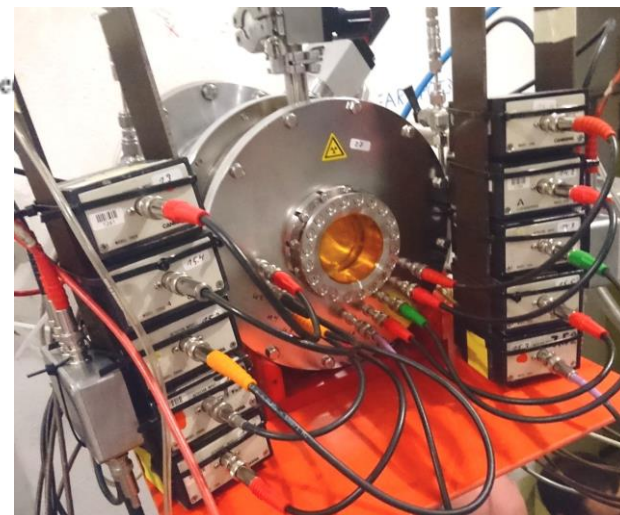
Contribution	Uncertainty (average)	Single deposit
^{235}U mass fraction	0.0014 %	0.0014 %
^{235}U mass per unit area	0.2 %	0.6 %
^{235}U effective density correction k_U	0.6 %	1–2.5 %
Zero-bias efficiency	1.3 %	1.1–1.3 %
Efficiency, extrapolation below thr.	3 %	2–4.5 %
Dead-time correction k_T	0.2 %	0.04–0.2 %

Ref.: E. Pirovano *et al.* JINST **18** (2023) P11011

Harwell FC H19 (200 mg ^{235}U)



n_TOF FC (32.7 mg ^{235}U)



Fission Detectors: PPAC

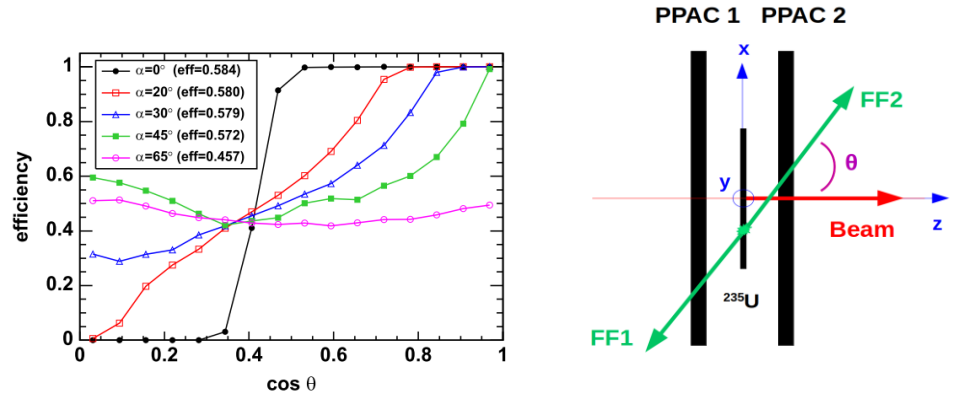
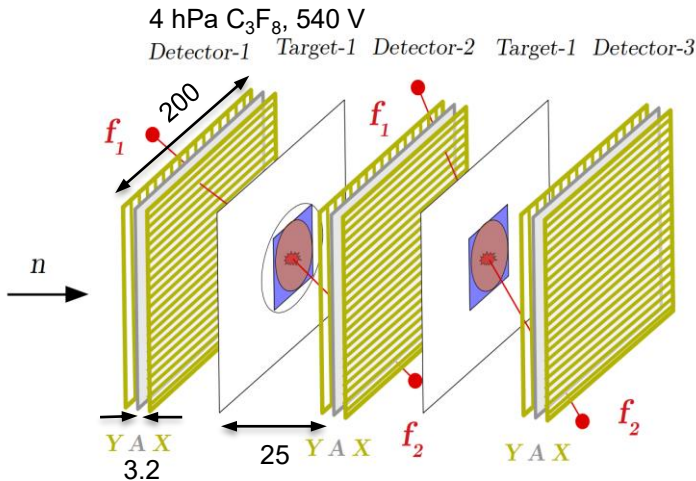


Fig. 4. Simulated detection efficiency for different values of the α angle between the normal to the detectors and the neutron beam direction. The total detection efficiency for each case is indicated in the legend, with a statistical uncertainty of ± 0.003 in all cases.

Ref.: D. Tarrio et al., NIMA 743 (2014) 79



Parallel Plate Avalanche Counter:

- Ionization chamber operated with gas amplification
- **Fast timing** for heavy ions and FF's
- Transparent backings (2 μm Al): detect both FF's
 \Rightarrow **excellent identification of fission events**
- Thin segmented electrodes (1 – 2 μm Mylar)
 \Rightarrow **insensitive to γ -flash**
- Spatial resolution by delay-line readout
- NB: **efficiency depends on the projectile angle!**

TOF Spectrometry with Frame Overlap

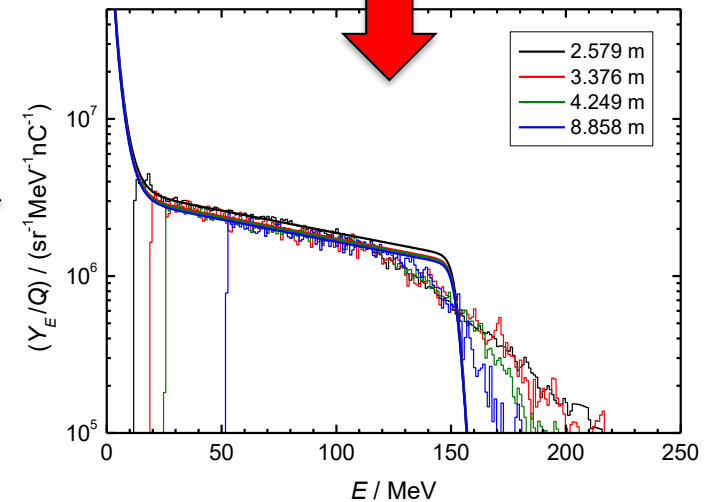
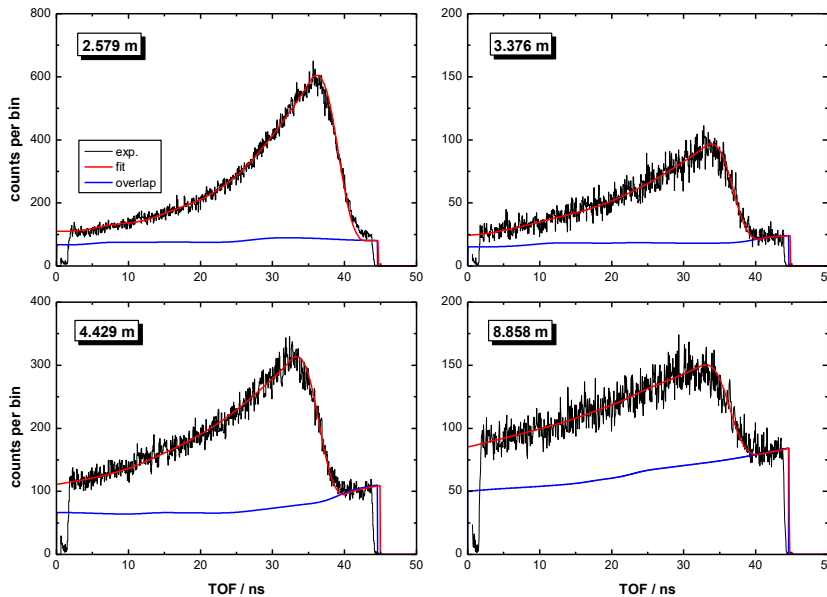
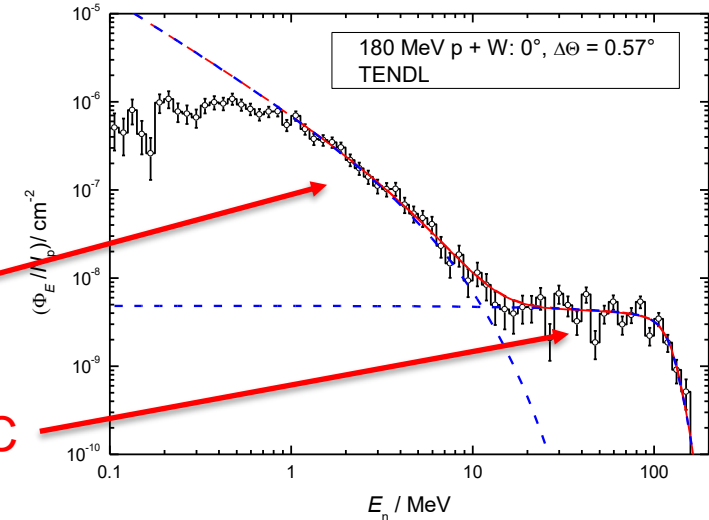
Difficult cases for TOF measurement:

- Broad energy distributions
- Short flight paths
- High repetition frequency

⇒ Combination of:

- Model calculations: **MCNPX**
- Measurements at several distances: **^{238}U -FC**

‘Atmospheric’ thick-target spectrum @ TSL

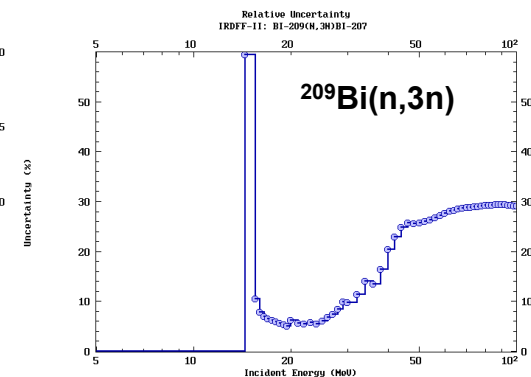
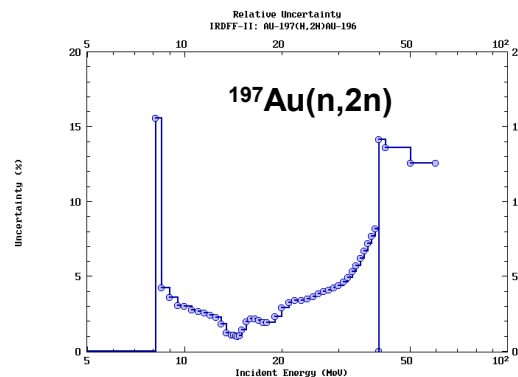
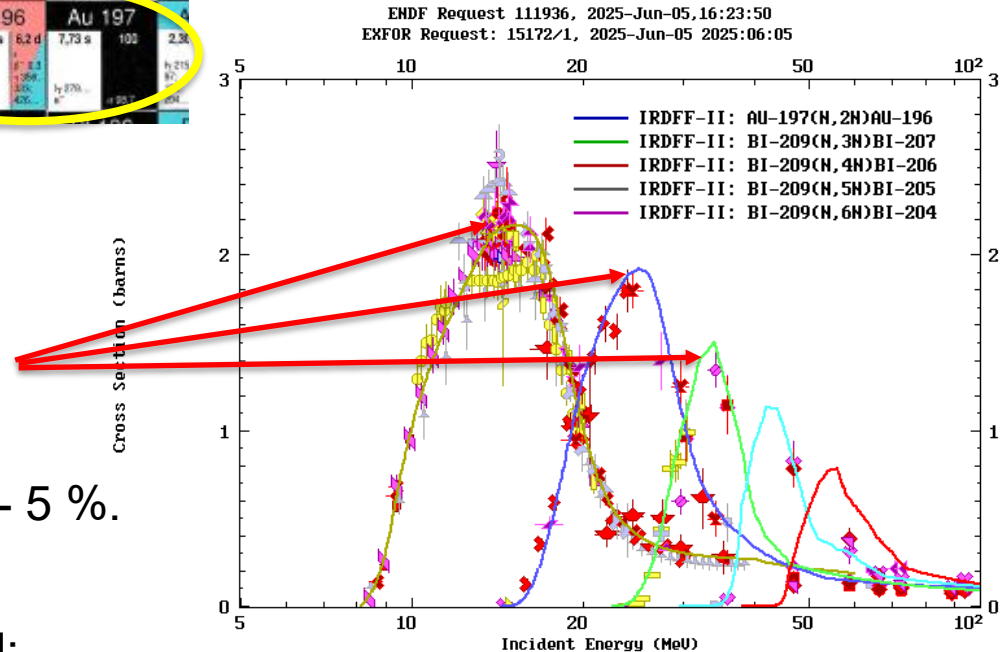


Alternatives to TOF: Spectrometry with Activation Foils

(n,xn) reactions with mono-isotopic samples: $^{197}\text{Au}(n,2n) + ^{209}\text{Bi}(n,xn)$



- $\sigma(E_n)$ distributions for the (n, x_n) channels are well localized.
- Evaluated XS uncertainty: 2 % - 5 %.
Few exp. data for $x > 4$!
- Few-channel unfolding required:
Uncertainty depends on the available pre-information!
- Interesting alternative to TOF for radiation hardness testing etc.



Beam Profile Monitors: Image Plates

Simple solution: image plate covered by a PE layer

Fujifilm IP BAS-MS-1: $^*Ba:F:Br:I$ phosphor in polyurethane matrix

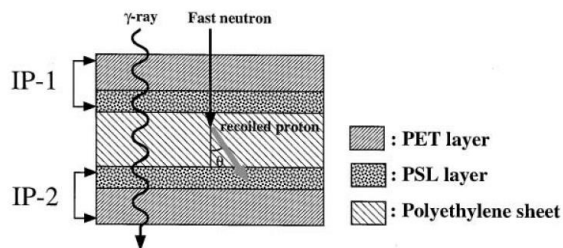
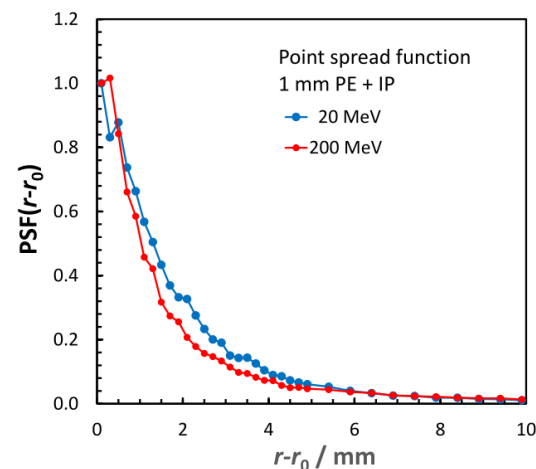
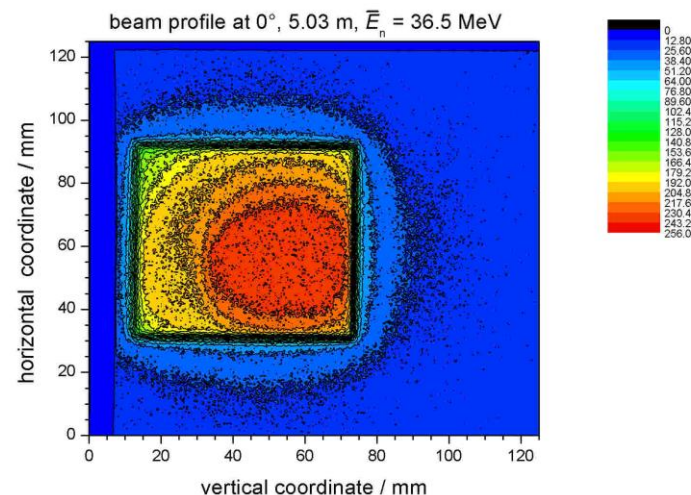
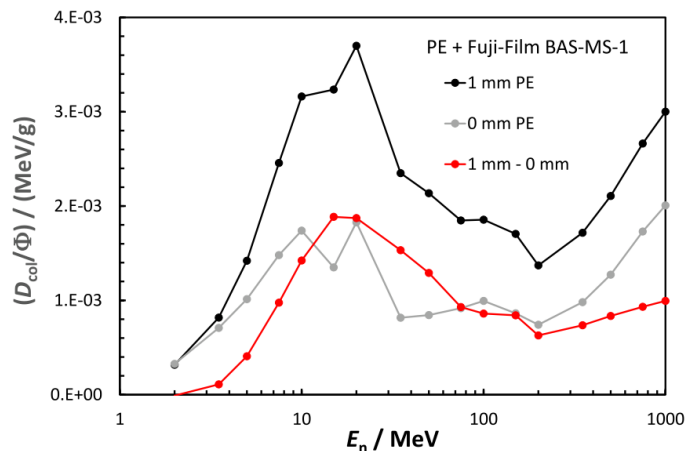


Fig. 1. Arrangement of imaging plates and a polyethylene sheet for FNR.

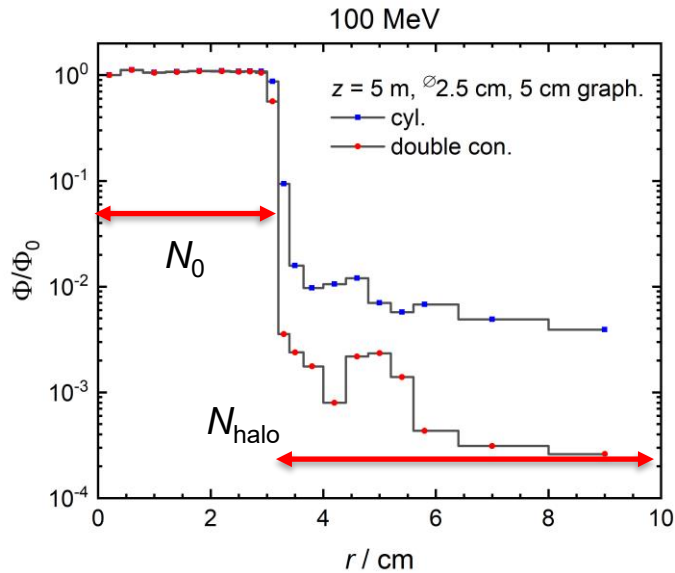
Ref.: M. Matsubayashi et al., NIMA 463 (2001) 324



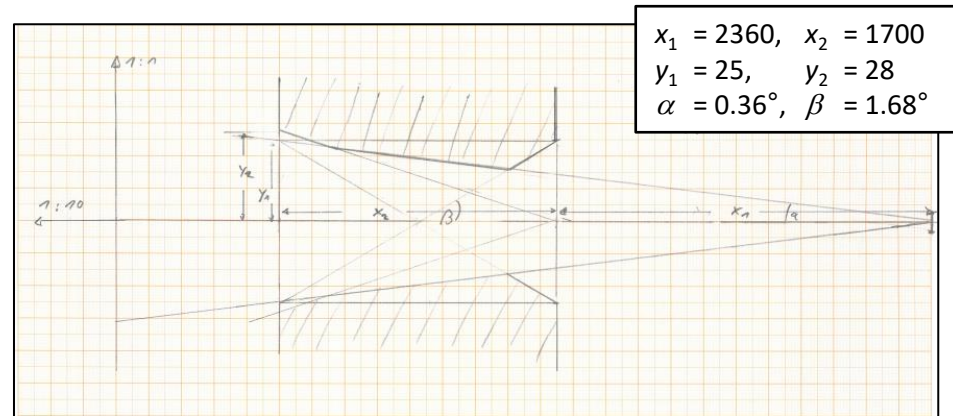
High sensitivity: $\approx 30 \text{ min per exposure}^1)$
Main disadvantage: no energy discrimination!

¹⁾ iThemba LABS: $^7\text{Li}+p$ @ 8 mm Li, $I_p = 5 \mu\text{A}$, $d = 8 \text{ m}$

Collimator Design: Neutron Penumbra



Optimized collimator shape: truncated cones



Neutron halo produced by scattering of neutrons inside the collimator opening:

- Optimization reduced N_{halo}/N_0 by a factor of five!
- Relevant for the calibration of large devices using the scanning technique (REM Counters, Bonner Spheres)

Ancillary Equipment: Intensity Monitors

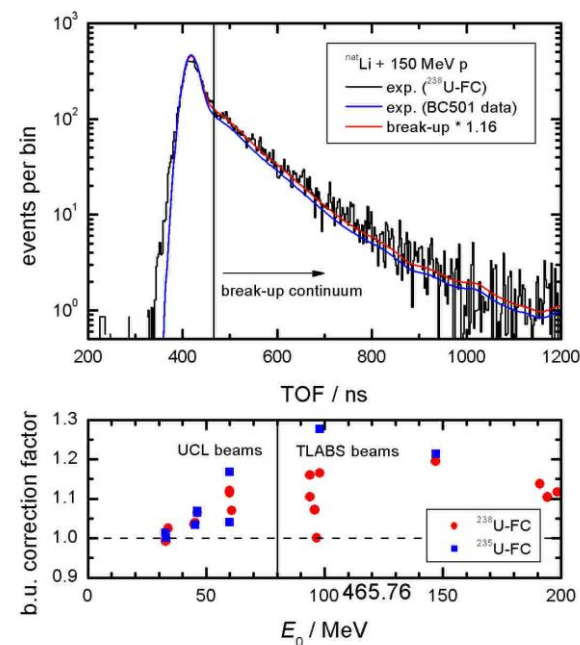
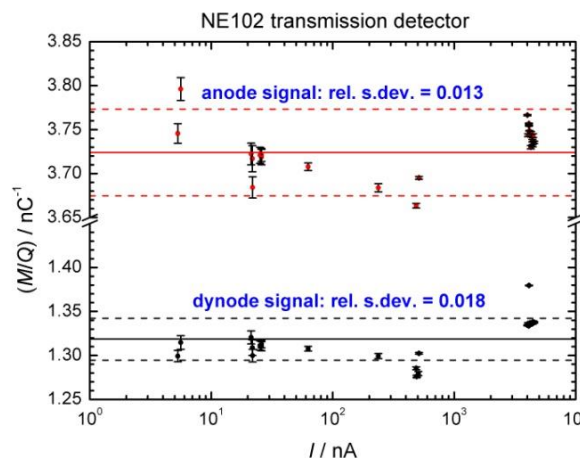
Efficiency of objects under test vary: $\delta\epsilon/\epsilon \leq 10^3!$

- Several monitors required to cover the dynamic range
- Stability of the neutron energy distribution: TOF – monitor
- Active gain stabilisation of PMTs required



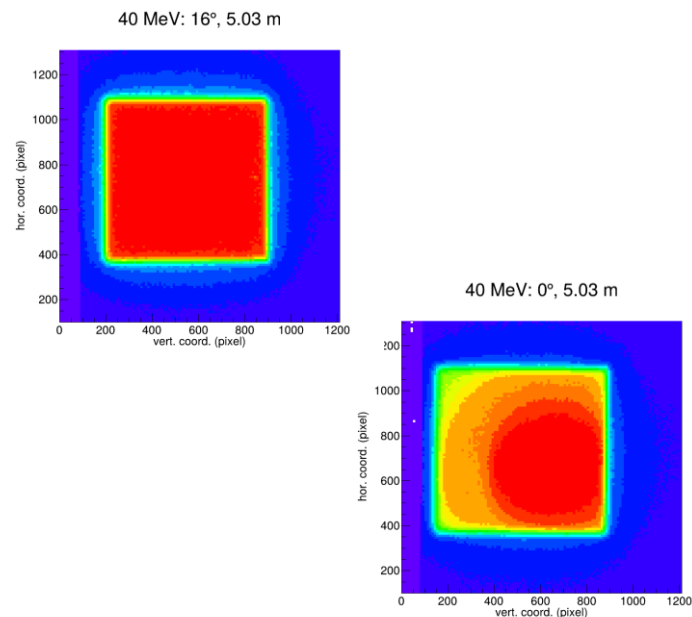
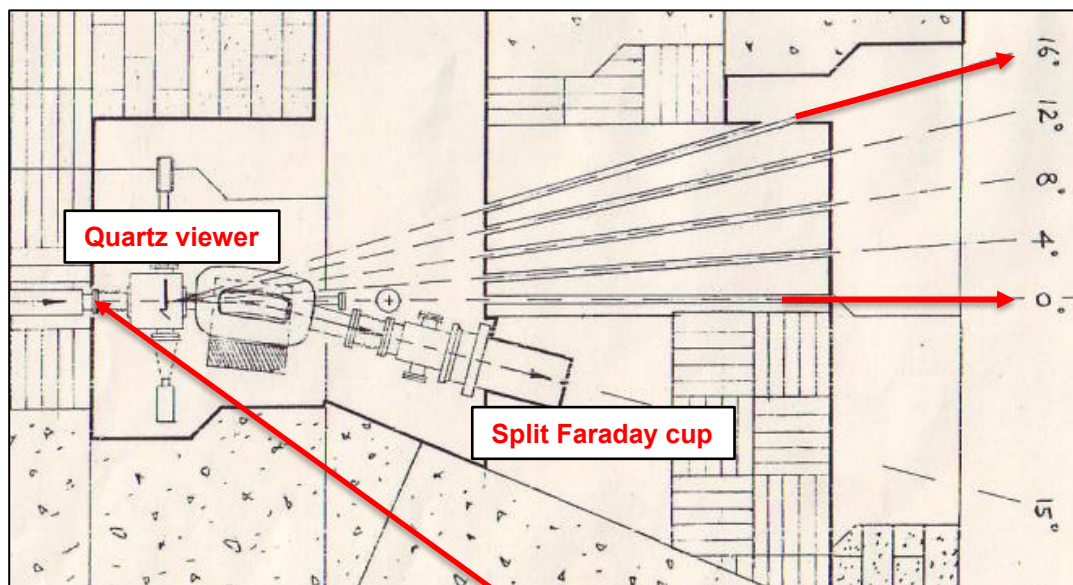
iThemba LABS facility

- beam current
- ^{238}U FC (200 mg)
- NE102 transmission det.



Ancillary Equipment: Proton Beam Diagnostics

iThemba LABS neutron beam facility:
 ${}^7\text{Li} + \text{p}$ (40 – 200 MeV)



Important issues:

- Moving proton beam on the Li target affects the neutron beam profile
 - Incomplete pulse suppression
- ⇒ Direct information for the operators

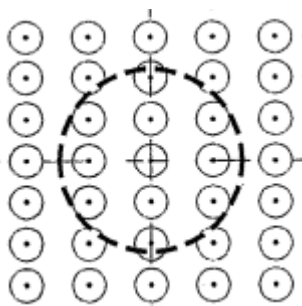
Urgent need: Retractable SEM grid for monitoring the proton beam profile!

Ancillary Equipment: Scanning Devices

Diameter of collimated neutrons beam: $d < 10$ cm

- Many objects under test are larger: Bonner spheres, REM counters ...
- Spot or step scanning techniques required to simulate a 'flat' field.
- Measure neutron 'current' J_E : $\Phi_E \approx J_E / A_{\text{scan}}$
- Minimize neutron halo!
- Time-resolved intensity monitors

Spot scan



Lissajous scan

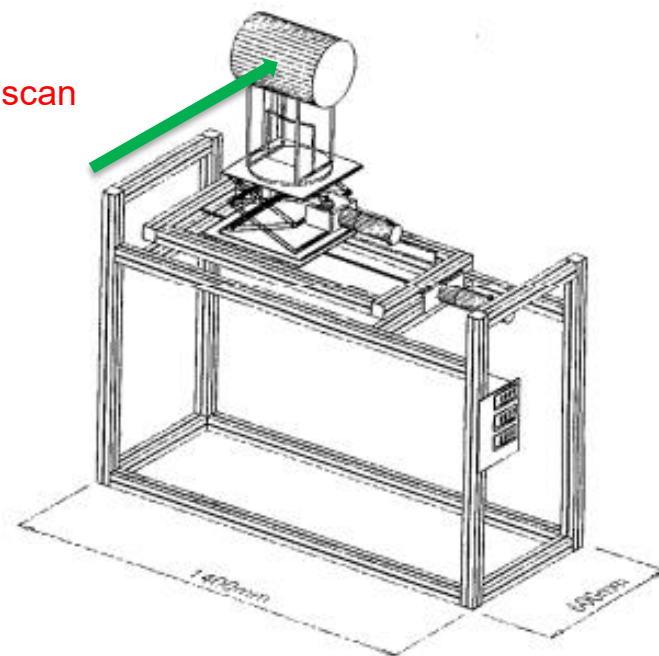
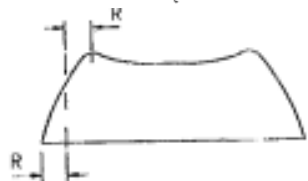
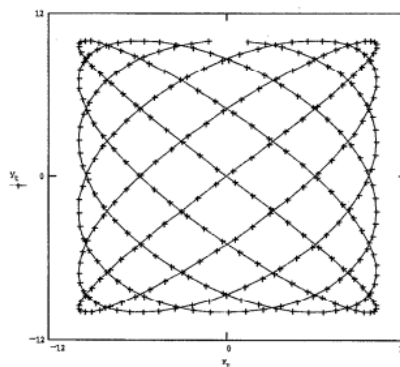


FIG. 9. Scanning system used for the calibration of the neutron rem counter.

Ref.: C. Birattari *et al.*, Rev. Sci. Instr. **66** (1995) 4198

Summary

Characterization of high-energy neutron reference beam relative to standard cross sections:

- $^1\text{H}(n,n)p$: RPTs with PE radiators and particle identification
- $^{235}\text{U}(n,f)$: PPFCs or PPACs with ^{235}U deposits
- Neutron energy distribution via TOF
- Spectrometry with activation foils for DC beams

Ancillary equipment for reference beam facilities:

- Neutron beam monitors: dynamic range $> 10^3$,
more than one system,
stability of the neutron energy distributions
- Proton beam diagnostics: beam profile and position,
pulse suppression
- Scanning devices for 'simulation' of large fields

Personal wish list:

- Extension of reference cross sections and MCNP libraries to 1 GeV
- Provide uncertainty for the $^1\text{H}(n,n)p$ DX !
- MCNP: Relativistic kinematics for light recoil particles

Acknowledgements

This is my very last talk in this business!

So, it's time to say 'thank you very much' to all former collaborators:

- Elisa Pirovano
- Mirco Dietz
- Quentin Ducasse
- Désirée Radeck
- Alice Manna
- Veronique Lacoste
- Nelson Magalotti
- Zina Ndabeni
- Tanya Hutton
- Peane Maleka
- Dieter Geduld
- Stefan Röttger
- Ricky Smit
- Andy Buffler
- Saalih Allie
- Volker Dangendorf
- Ulrich Schrewe
- Helmut Schuhmacher
- Hein J. Brede



... and many others!